INVESTIGATION OF EFFECT OF NOZZLE GEOMETRY ON SPRAY WITH A 3D EULERIAN-LAGRANGIAN SPRAY MODEL COUPLED WITH THE NOZZLE CAVITATING FLOW

Genmiao GUO[1], Zhixia HE[2*], Qian WANG[1], Zhaochen JIANG[1], Liang ZHANG[1]

[1]School of Energy and Power Engineering, Jiangsu University, China

[2]Institute for Energy Research, Jiangsu University, China

[*]Zhixia HE; E-mail: zxhe@ujs.edu.cn

A 3D Eulerian-Lagrangian spray model coupled with the nozzle cavitating flow was proposed to simulate the atomization and secondary break-up. The nozzle flow and near-field spray were simulated with the Volume Of Fluid (VOF) multiphase model. At a certain downstream location, where the spray is diluted, the Eulerian spray approach was switched to the conventional Lagrangian approach. This entire methodology was validated through the experimental data of liquid spray penetration under non-evaporating chamber conditions. The numerical simulations based on multi-scheme were implemented by this model to investigate the effects of nozzle geometry and configuration on the subsequent spray development.

Key words*: diesel engine; nozzle; X-rays; cavitating flow; primary atomization; spray model*

1. Introduction

The tiny nozzle in the high-pressure common rail injection system, connected to the fuel injection upstream and downstream spray atomization, has become one of the most key components of advanced diesel injection and combustion engineering. Ranz[1] has proposed the diesel engine nozzle spray atomization is associated with internal nozzle flow, and later numerous studies have verified the cavitation phenomenon will produce inevitably under the high injection pressure in the small orifice, which in turn influence the external spray breakup, fuel-air mixing processes, and emissions[2-4].

A number of scholars have carried out experimental and/or numerical investigations on the cavitation characteristics in the diesel orifice. Bergwerk[5] found that the discharge coefficient of the orifice is mainly dependent on the cavitation number and independent on the Reynolds number based on the experiments on simplified single-orifice acrylic nozzles. Mulemane et al.[6] performed experimental and numerical investigations to study the influence of operating parameters and critical injector design parameters on the dynamic performance of advanced high-pressure electronically controlled diesel injection systems. The needle lift characteristics show that the measured injection rate is a strong function of the injection pressure and the nozzle diameter. Sou et al.[7] studied the effects of nozzle geometries on cavitation in the orifice using two-dimension (2D) nozzles with various geometries. The research confirmed that the thickness of the cavitation zone increases with the contraction coefficient of the cross sectional area at upstream of the nozzle to that of the nozzle. He et al.[8] analyzed the effects of the needle lift, the inlet radius and the sac volume on the cavitating flow based on a testified cavitation model which was validated by the experimental data obtained from the

flow visualization experiment system. Numerical results clearly reveal the distribution of the cavitation zone. Margot et al.[9] conducted a comprehensive study on a three-dimension (3D) flow inside diesel injector-like geometries under a cavitation model implemented in a Computational Fluid Dynamics (CFD) code. Various numerical parameters were used to simulate cavitation under realistic diesel engine conditions and the results show that the cavitation model was able to predict the onset of cavitation, which were verified with experiments both on the injection rate and the occurrence of choked flow.

However, due to the complex interaction of vortices, cavitation and turbulence, the CFD modeling remains one of the best techniques to explore and understanding the multi-phase flow. The precise nozzle geometrical parameters provide a reliable basis for the numerical simulation, but it is rather difficult to obtain the internal accurate geometric structure by non-destructive traditional methods, which can be solved effectively by the use of synchrotron radiation technology. Lebas et al. [10] studied the dense spray region by implemented a 3D model for atomization based on an Eulerian single-phase approach in a professional CFD code via AVL FIRE, which has been proved that can improve the description of the primary break-up. Hoyas et al.[11] captured many of the most important characteristics of the spray, such as the penetration and the axial velocity, using 2D simulations based on the Eulerian-Lagrangian spray atomization model via STAR-CD. As can be seen in many commercial software and open source codes, the most efficient and widely-applied approach is the Lagrangian-Droplet-Eulerian-Fluid (LDEF) method. Instead of solving the liquid phase as a partial-differential-equation based continuum, such as in the LDEF method treats the liquid as discrete particles. These particles are assumed to be negligible in volume and are superimposed on the continuous gas phase as material points. At the nozzle exit, liquid fuel is injected as discrete “blobs”, and a linear stability based phenomenological model is applied to account for the primary breakup [12]. In spite of its efficiency, the accuracy in the near-nozzle region is low, due to the fact that the liquid fuel is actually a continuum as observed in both experiments and Direct Numerical Simulation (DNS). As a result, the model's connection to the nozzle flow is inherently weak, despite some efforts to model the unresolved near-nozzle physics and to consider the effects of in-nozzle cavitation and turbulence on the primary breakup[13,14].

In this paper, the accurate three-dimensional geometric structure of the real nozzle was measured as a basis for numerical simulations. VOF method was used to simulate the internal nozzle flow and the primary breakup near the outlet of the nozzle orifice, then the traditional LDEF method was set in the dilute spray region of the nozzle downstream. And then, in order to validate this simulation model, experimental data compared to were performed. Finally, the effects of different injector geometries on the spray angle, penetration, and particle size distribution under different injection pressures were investigated.

2. Synchrotron Radiation Measurement of Nozzle Structure

The Synchrotron Radiation Facility (SRF) applied in this paper can provide a variety of synchrotron radiations from infrared light to hard X-ray. During the measurements, 55keV electrons penetrated the front of injector and exposure to scintillation crystal, then the X-ray absorption image can be captured by the Charge Coupled Device (CCD) camera in the front of injector. In the orifice measurement process, the injector seated on the sample rotation stage revolved 180°at the speed of 1.8°/s. In this process, an X-ray absorption image were captured every 0.2° with 10s exposure time

and 9mm spatial resolution by the CCD camera. Much detailed information about the measurement was shown in Table 1. The photon flux density of the SRF is 1×10^{10}phs • s^{-1} • mm^{-2} at 20keV and the maximal beam size can arrive 48mm (H)×5mm (V) at 20keV, where the distance between the light and the sample is 30m.

TAB. 1 Main parameters of the experiment.

Energy range	8~72.5keV
Energy resolution	$\leq3\times10^{-3}$
Photon flux density	1×10^{10}phs • s^{-1} • mm^{-2}
Maximal beam size	48mm (H)×5mm (V)

Fig. 1(a) shows the measurement results of eight orifices of the tested nozzle, and the Table 2 gives more detailed information about the eight different orifices. In order to simplify the calculation, we just choose one orifice (eg. the 4th orifice) of the eight different ones to study. Fig. 1(b) shows the slice of the 4th orifice of the eight different orifices which is the basis of the consequent nozzle flow and spray simulation. The left part of the axis is the mirror image of the 4th orifice which is at the right part of the axis. It is can be seen that both the inlet diameter (D_{in}) and the outlet diameter (D_{out}) of the 4th orifice are about 183μm, and the orifice length (L) is about 598μm, while the orifice inlet top curvature radius (R_a) and the orifice inlet bottom curvature radius (R_b) are about 65μm and 33μm, respectively. And the spray angle (θ) between orifice axis and injector axis is 62.9°.

TAB. 2 Measurement results of eight different orifices.

NO.	D_{in} (μm)	D_{out} (μm)	L (μm)	R_a (μm)	R_b (μm)	θ (°)
1	184	183	589	70	35	62.8
2	181	184	602	62	30	62.3
3	180	182	595	58	28	62.5
4	183	183	598	65	33	62.9
5	185	184	588	61	32	63.1
6	182	185	595	62	31	62.6
7	181	183	598	68	34	62.8
8	185	182	603	70	33	62.7

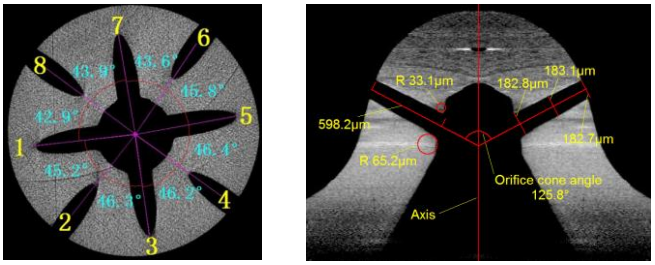

(a) (b)

FIG. 1: The slice of injector in different directions. (a) The measurement results of eight orifices of the tested nozzle, and (b) The slice of the 4th orifice of the eight different orifices.

3. Spray Simulation Coupled with Nozzle Flow

3.1. Models of hydrodynamic cavitation

In this paper, VOF multiphase model was employed to deal with the internal cavitating flow and the near-field dense spray. VOF model is mainly based on transportation of the volume fraction, that is, a source term representing phase transition which is governed by the difference between the local pressure and the vapor pressure. According to the vapor fraction transport equation, cavitation is assumed to occur due to the bubble nuclei or micro bubbles in the liquid, which can grow or collapse with the changing of the surrounding conditions. Moreover, the growth and collapse of the bubbles are taken into account according to the Rayleigh's simplified bubble dynamics equation[15].

The bubble distribution can be described by a single scalar field which is the vapor volume fraction α_v, because it is assumed that all vapor bubbles in the control volume have the same radius and a homogenous distribution. Also, assuming that only exists a single liquid phase, and the bubbles will occupy the corresponding control volume when the cavivation take place. Eq. (1) is a description for the relationship between the vapor volume fraction α_v and the average vapor bubble radius R:

$$\alpha_v = \frac{V_v}{V} = \frac{N_{bub}\frac{4}{3}\pi R^3}{V_l + V_v} = \frac{n_0 V_l \frac{4}{3}\pi R^3}{V_l + n_0 V_l \frac{4}{3}\pi R^3} = \frac{n_0 \frac{4}{3}\pi R^3}{1 + n_0 \frac{4}{3}\pi R^3} \tag{1}$$

Where, V_v and V_l are the volume occupied by the vapor phase and liquid phase respectively, and V is the total control volume; N_{bub} is the number of vapor bubbles in the control volume; n_0 is the number density of bubbles per volume of liquid.

The vapor volume fraction α_v in the control volume will change with the convective transport and bubbles' growth or collapse. The Eq. (2) describing the transport of α_v based on the assumption that the vapor density is much smaller than that of the liquid density:

$$\frac{d}{dt}\int_V \alpha_V dV + \int_S \alpha_V (v - v_s)\cdot dS = \int_V \frac{n_0}{1 + n_0 \frac{4}{3}\pi R^3}\frac{d}{dt}(\frac{4}{3}\pi R^3) dV \tag{2}$$

The right side of Eq. (2) is the cavitation bubble growth rate of the model, which can be obtained by the observation on the Lagrangian of a cloud of bubbles and the conventional bubble dynamic observation of a single bubble in an infinite stagnant liquid respectively. This analysis results is the extended Rayleigh - Plesset equation:

$$\frac{d}{dt}\int_V \alpha_v dV + \int_S \alpha_v (v - v_s)\cdot da = \int_V \frac{n_0}{1 + n_0 \frac{4}{3}\pi R^3}\frac{d}{dt}\left(\frac{4}{3}\pi R^3\right) dV \tag{3}$$

Where, P_{sat} is the saturation pressure corresponding to the temperature at the bubble surface, P_∞ is the pressure of the surrounding liquid; ρ_l and μ_l are the liquid density and viscosity respectively, and σ is the surface tension coefficient.

The precise geometry structure of the 4th orifice of the nozzle obtained by synchrotron radiation measurement was used to simulate the nozzle flow. Fig. 2 was the structure and the mesh used for nozzle flow simulation, and the total grid number chosen was 102529 based on the grid independence tests. All simulations were made with the standard $k-\varepsilon$ turbulence model with standard wall functions. The solver applied was based on the pressure correction and the algorithm applied was SIMPLEC. What the discretization of the $k-\varepsilon$ turbulence model equations used was the upwind differencing scheme and the cavitation model used was based on the Rayleigh equation and associated

with the rate of change of the bubble radius depended on the local pressure, where the density of liquid and vapor were constant and there was no slip between the bubbles and the liquid.

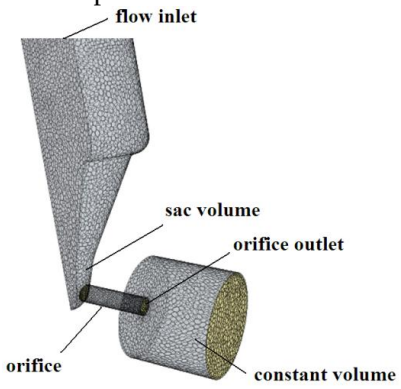

FIG. 2: The mesh of injector used (the 4th orifice) for nozzle flow simulation.

3.2. Eulerian-Lagrangian spray model

The near-field dense spray was simulated with the VOF multiphase model the same as the flow in the orifice. The atomization of diesel sprays is modeled as a turbulent mixing process of the liquid fuel with the ambient gas. At a certain downstream location, where the spray is diluted, this Eulerian spray approach was switched to conventional Lagrangian approach which thought the droplet parcels as the control liquid volumes in the computational domain of spray and could depicted the mutual effects between droplets and gas, evaporation and break-up and so on. Fig. 3 is the diagram for the Eulerian-Lagrangian coupled spray model, which gives the thought of this spray model clearly.

The conventional Lagrangian spray was simulated by STAR - CD. Theoretical studies provided a criterion for the onset of break-up and an estimate of the stable droplet diameter ($D_{d,\,stable}$) and the characteristic time scale τ_b of the break-up process, simultaneously. The break-up rate of the spray can be calculated by Eq. (4):

$$\frac{dD_d}{dt} = -\frac{\left(D_d - D_{d,stable}\right)}{\tau_b} \tag{4}$$

Where, D_d is the instantaneous droplet diameter.

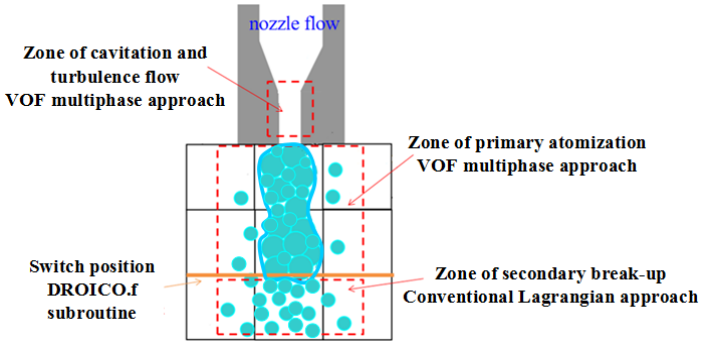

FIG.3: Zones division of coupled spray model.

Instability of the spray is determined by a critical value of the Weber number (*We*) and the droplet Reynolds number (*Re*), Eq. (5) and Eq. (6):

$$We = \frac{\rho\left|u - u_d\right|^2 D_d}{2\sigma_d} \geq C_{b1} \tag{5}$$

$$\mathrm{Re} = \frac{\rho|\mu - \mu_d|D_d}{\mu} \tag{6}$$

The criterion for the onset of this Stripping break-up regime is

$$\frac{We}{\sqrt{\mathrm{Re}_d}} \geq C_{s1} \tag{7}$$

The characteristic time scale for this Stripping break-up regime is

$$\tau_b = \frac{C_{s2}}{2}\left(\frac{\rho_d}{\rho}\right)^{1/2}\frac{D_d}{|u - u_d|} \tag{8}$$

Here, the empirical coefficient C_{s1} is the value 0.5 and C_{s2} is in the range from 2 to 20.

3.3. Switch method of the Eulerian- Lagrangian model

The calculation data of injector flow (cavitation and turbulence) delivered to downstream conventional Lagrangian spray simulation by the mean of subroutine in STAR - CD, which contained 13 return values. Fig. 4 shows the detail information of these parameters. The velocity (magnitude and direction) and density of the upstream Euler flow were made as the initial conditions of the downstream applying the conventional Lagrangian approach.

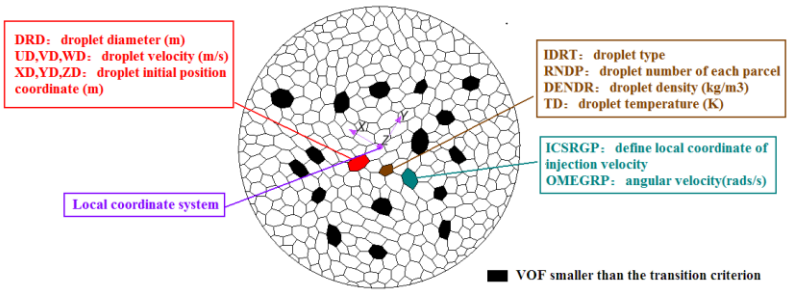

FIG.4: The detail information of return values.

It was assumed that the spray zones, where the distance to orifice outlet is longer than 2mm, were dilute spray zone. The simulation cells of switch location cross-section, whose liquid volume of fraction was bigger than 0.5, were chosen as the fuel injector cells. The positions of these cells were considered as the position of the droplet parcels injected and the velocities of these cells were considered as the initial velocities (magnitude and direction) of droplets. So this model could simulate the spray angle and it was not needed to give previously. The initial droplet size was determined by the fuel liquid volume of fraction. The diameters of fuel droplets were proportional to the volume of fraction value of fuel liquid. It was assumed that the initial size was the orifice diameter multiply by corresponding scale factor[16].

4. Validation of Eulerian-Lagrangian spray model

Traditional spray model means simulating the spray directly without coupled the nozzle flow, Eulerian-Lagrangian coupled spray model on STAR - CD that is the model applied in this paper, and coupled spray model on FIRE[17] were simulated based on the 4th nozzle. From Fig.5, it can be easily found that the simulation data of coupled spray were much closer to the experimental data[17] than traditional spray model, which verified the accuracy of the coupled spray mode. Meanwhile, the data

obtained from the coupled spray model on FIRE is consistent with that got from the Eulerian - Lagrangian coupled spray model on STAR - CD, which justifying the subprogram compiled coupled the cavitating flow to spray model was feasible in some degree, and the calculation precision of model proposed in this paper can meet the current mainstream commercial software. What obtained from the two kind of coupled spray mode further verified the accuracy of the Eulerian-Lagrangian coupled spray model.

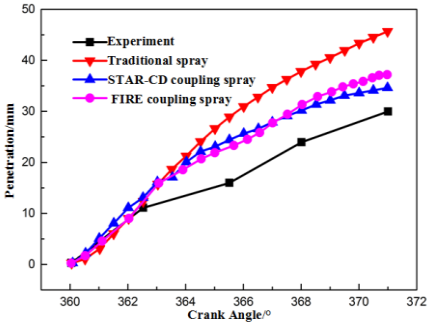

FIG.5: Tip penetrations of traditional spray, coupled spray and experiment data.

Though the predicted results of the coupled spray mode were higher than the experimental, results obtained from spray simulations which coupled with internal cavitating flow were superior to that traditional spray model which did not consider the influence of internal cavitating flow. For the slight unavoidable differences between predicted and experimental results, the errors in the measurement of spray penetration distance and simplification of the boundary conditions in spray simulation were regarded as the dominant causes.

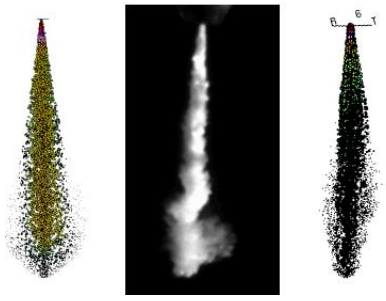

(a)Traditional spray(b)Experiment (c)STAR-CD coupled spray

FIG. 6: The distribution of the spray droplet diameter obtained by traditional spray, experiment and coupled spray.

Based on the verification above, numerical simulation was conducted with the Eulerian - Lagrangian coupled spray model on STAR - CD. The conditions were same as the experiment by Verhoeven et al.[18], that is, the injection pressure is 50MPa, and the back pressure is 2MPa. As shown in Fig. 6 is the distribution of the spray droplet diameter obtained by different methods, though the Eulerian - Lagrangian coupled spray model on STAR - CD simulations result was less than the traditional spray model, the spray penetration was much closer to the experiment, especially the spray near the outlet of the orifice because of considering the flow inside the nozzle.

5. Effects of different injector geometries on the spray characteristics

According to the study[8], the injector geometries have important effects on the spray. In this paper, using the above verified coupled spray model, the multi-scheme numerical simulations were

carried out for the different nozzle geometry parameters, such as the ratio of nozzle orifice length to diameter(L/D), orifice entrance curvature radius (R) and the different nozzle configurations like the standard (STD) type, valve covered orifice (VCO) type, and the improved (IMPROVED) type, to analyze the effects of the nozzle geometries on the subsequent spray.

5.1. Effects of the l/d and r on the spray characteristics

The nozzle configuration was the STD type, and the pressure at the inlet was 50MPa and the back pressure was 0.5MPa.

When studying the effect of the different L/D on the spray characteristics, the orifice entrance curvature radius (R) is 0, and the orifice diameter (D_d) is 0.228 mm. The simulation results for different ratios of nozzle orifice length to diameter (L/D = 2, 3 and 4) were shown in Fig. 7. The spray tip penetration is increased with the ratio of length to diameter increased, and the sauter mean diameter (SMD)would increase.

As for investigating the effect of the orifice entrance curvature radius (R) on the spray characteristics, the ratio of orifice length to diameter (L/D) was 4. Fig.8 showed the simulation results for the three different kinds of orifice entrance curvature radius, that is R =0, R =0.0228mm and R =0.0456mm. It presented that if the entrance curvature radius decreased, the spray tip penetration and the SMD were decreased rapidly. And it could find that both at R =0.0228 and R =0.0456mm the spray tip penetration and the SMD were nearly similar, but had a large distinction compared to the condition of R =0. It could be supposed that the existence of entrance curvature radius may reduce the cavitation inside the orifice.

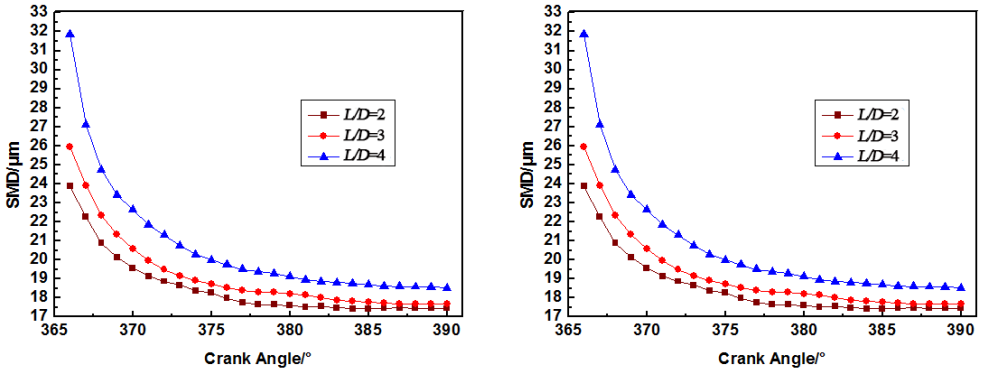

FIG.7: Spray tip penetration and SMD for L/D = 2, 3 and 4.

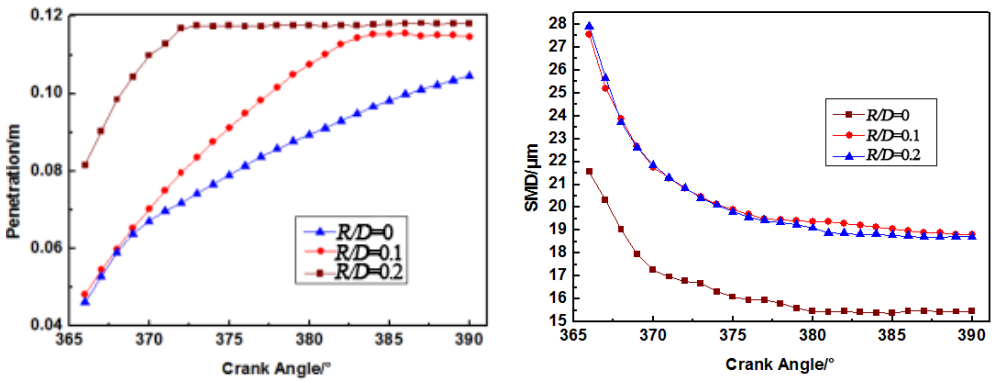

FIG. 8: Spray tip penetration and SMD for R = 0, 0.0228 and 0.0456mm.

5.2. Effect of the types of sac volume on the spray characteristics

The main difference of the STD, VCO, and IMPROVED type nozzle is the relative location of the orifice and the needle valve seat, so there are different sac volume, as shown in Fig. 9. The orifice of STD type is under the needle valve seat with a large sac volume, and the orifice of VCO type nozzle is above the needle valve seat nearly without sac volume, and also the orifice of IMPROVED type is above the needle valve seat, but it has a sac volume a bit smaller than the STD type.

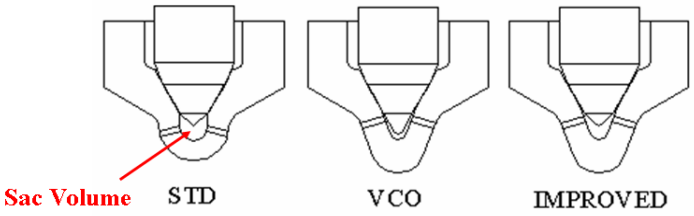

FIG. 9: Three types of nozzle with different sac volume.

For these three different models, they had the same boundary conditions and orifice geometry. Injection pressure was 50MPa and the back pressure was 0.5MPa. The calculation results were shown in Fig. 10. At the early stage of the injection, the tip penetration of the three different types were similar, while at the end stage of injection, the VCO nozzle had the longest penetration and the smallest value of SMD. Considering of nozzle cavitating flow comprehensively, from the aspect of spray tip penetration and SMD, IMPROVED nozzle could acquire better spray characteristics.

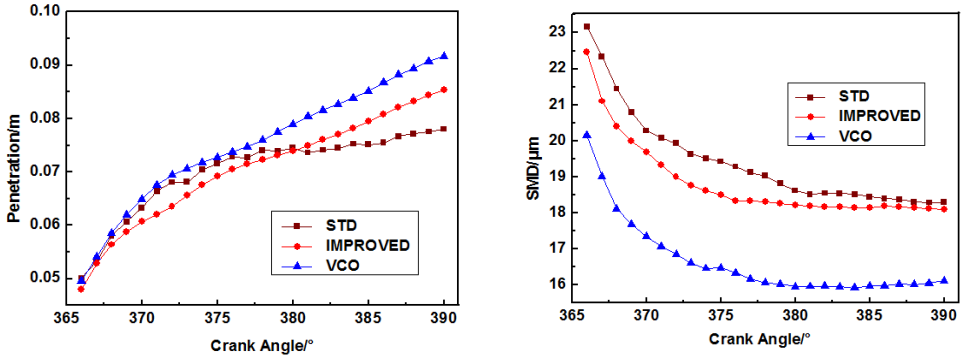

FIG. 10: Spray tip penetration and SMD of three different types of nozzle.

6. Summary and Conclusions

In this paper, a three-dimensional high-precision structure model of nozzle geometry was obtain used the X-ray phase contrast imaging measurement, which was helpful to establish the CFD model of nozzle more exactly.

The model proposed in this paper adopted the VOF method to simulate the internal nozzle flow and the near-field dense spray, then used the original position of the traditional LDEF method for the nozzle downstream. The velocity (magnitude and direction) and density of the upstream Euler flow were made as the initial conditions of the downstream applying the conventional Lagrangian approach. Comparing the visual spray experiment data and numerical results, it was verified that the spray model coupled with cavitating flow in nozzles was more accurate than the traditional spray model widely used nowadays.

The multi-scheme numerical simulations indicated that the nozzle structure has an important effect on the spray characteristics. The spray tip penetration is increased with the ratio of length to diameter increased, and the SMD would increase. The existence of entrance curvature radius may

reduce the cavitation inside the orifice, and causing a larger value of the tip penetration and the SMD. Considering of nozzle cavitating flow comprehensively, from the aspect of spray tip penetration and SMD, IMPROVED nozzle could acquire better spray characteristics. The simulation results supply the theoretical foundation for the optimization design of the injector.

Acknowledgments

This work was supported by the National Natural Science Foundation of China (No.51176066, No.51276084), Six Talent Peaks Project of Jiangsu Province (2013-JNHB-017).

Nomenclature and unit

D	diameter of orifice, m
L	length of orifice, m
L/D	length to diameter of orifice
R	curvature radius, m
V	volume, m^3
N_{bub}	number of vapor bubbles
α	volume fraction
P_{sat}	saturation pressure, Pa
P_{∞}	surroundingpressure, Pa
ρ	density, kg/m^3
μ	dynamic viscosity, Pa·s
σ	surface tension of the fluid, N/m
θ	spray angle, °
D_d	droplet diameter, m
τ_b	characteristic time scale, s
We	Weber number
Re	Reynolds number
C_{s1}, C_{s2}	empirical coefficient
R_a, R_b	the orifice inlet top and bottom curvature radius, m
SMD	Sauter Mean Diameter, m
2D, 3D	two/three dimension
VOF	Volume Of Fluid
CFD	Computational Fluid Dynamics
DNS	Direct Numerical Simulation
CCD	Charge Coupled Device
SRF	Synchrotron Radiation Facility
STD	Standard
LDEF	Lagrangian-Droplet-Eulerian-Fluid
IMPROVED	improved

Subscript

l	liquid phase
v	vapor phase
d	droplet
in	upstream location of a nozzle
out	nozzle hole outlet

References

[1] Ranz, W.E., Some experiments on orifice sprays. The Canadian Journal of Chemical Engineering, vol 36, pp. 175–181, 1958.

[2] Molina, S., Salvador, F.J., Carreres M., and Jaramilloet, D., A computational investigation on the influence of the use of elliptical orifices on the inner nozzle flow and cavitation development in diesel injector nozzles. Energy Convers Manage, vol. 79, pp. 114–127, 2014.

[3] Monhan, B., Yang, W., and Chou, S.K., Development of an accurate cavitation coupled spray model for diesel engine simulation. Energy Convers Manage, vol. 77, pp. 269–277, 2014.

[4] Shinjo, J., and Umemura, A., Detailed simulation of primary atomization mechanisms in diesel jet spray, *International Journal of Multiphase Flow*, vol. 36, pp. 513-532, 2010.

[5] Bergwerk, W., Flow pattern in diesel nozzle spray orifices. *Proceedings of the Institution of Mechanical Engineers*, vol. 173, pp. 655-660, 1959.

[6] Mulemane, A, Han, J.S., Lu, P.H., Yoon, S.J., and Lai, M.C., Modeling dynamic behavior of diesel fuel injection systems, *SAE Technical Pape*r, 2004-01-0536, 2004.

[7] Sou, A., Maulana, M.I., Isozaki, K., and Hosokawa, S. Effects of nozzle geometry on cavitation in nozzles of pressure Atomizers, *Journal of Fluid Science and Technology*, vol. 3, no. 5, 2008.

[8] He Z.X., Zhong W.J., Wang Q., Jiang Z.C., and Shao Z., Effect of nozzle geometrical and dynamic factors on cavitating and turbulent flow in a diesel multi-orifice injector nozzle, *International Journal of Thermal Sciences*, vol. 70, pp. 132-143, 2013.

[9] Margot, X., Hoyas, S., Gil, A., and Patouna, S., Numerical modelling of cavitation: validation and parametric studies, *Engineering Applications of Computational Fluid Mechan*ics, vol. 6, no. 1, pp. 15-24, 2012.

[10] Lebas, R., Blokkeel, G., Beau, P.A., and Demoulin, F.X., Coupling Vaporization model with the Eulerian-Lagrangian spray atomization (ELSA) model in diesel engine conditions, *SAE Technical Paper*, 2005-01-0213, 2005.

[11] Hoyas, S., Pastor, J.M., Khuong-Anh, D., Application and evaluation of the Eulerian-Lagrangian spray atomization (ELSA) model on CFD diesel spray simulations, *SAE Technical Paper*, 2011-37-0029, 2011.

[12] Vallet, A., Burluka, A.A., and Borghi, R., Development of a Eulerian model for atomization of a liquid jet, *Atomization and Sprays*, vol. 11, pp. 619-642, 2001.

[13] Shi, J., Guerrassi, N., Dober, G., Karimi, K., and Meslem, Y., Complex physics modelling of diesel injector nozzle flow and spray supported by new experiments, *in THIESEL, Valencia, Spain*, 2014.

[14] Som, S., and Aggarwal, S.K., Assessment of atomization mechanisms in diesel engine simulations, *Atomization and Sprays*, vol. 19, pp. 885-903, 2009.

[15] Martynov, S., Numerical simulation of cavitation process in diesel fuel injectors, *Doctoral dissertation, University of Brighton, Brighton*, 2005.

[16] Reitz, R.D., and Diwakar, R., Structure of high pressure fuel spray, *SAE Technical Paper*, 870598, 1987.

[17] Liu, J.Y., Study on spray simulation coupled with nozzle cavitating flow in high-pressure common rail injection system, *Master thesis, University of Jiangsu, China*, 2012. (in Chinese)

[18] Verhoeven, D., Vanhemelryck, J.L., and Baritaud, T., Macroscopic and ignition characteristics of high-pressure sprays of single-component fuels, *SAE Technical Paper*, 981069, 1998.

Paper submitted: September 4, 2016

Paper revised: October 26, 2016

Paper accepted: October 27, 2016